Composites Science and Technology 162 (2018) 131–139

Contents lists available at ScienceDirect

Composites Science and Technology

journal homepage: www.elsevier.com/locate/compscitech

Self-assembled montmorillonite–carbon nanotube for epoxy composites with superior mechanical and thermal properties

Shaohua Zeng, Mingxia Shen*, Lu Yang, Yijiao Xue, Fengling Lu, Shangneng Chen

College of Mechanics and Materials, Hohai University, Nanjing 211100, China

ARTICLE INFO

Keywords:
A. Polymer-matrix composites (PMCs)
A. Carbon nanotubes
B. Surface treatments
B. Interface

ABSTRACT

A hybrid nanostructure consisting of montmorillonite – multi-walled carbon nanotube (Mt – MWCNT) was designed and assembled, and further used as reinforcing nanofillers for preparing epoxy-based composites. It was found that Mt could efficiently resist microcrack extension and hinder thermal transfer while MWCNTs anchored on the Mt nanosheets could facilitate the stress and heat transfers and provide mechanical interlocking with the epoxy matrix. Making use of the synergistic effect of Mt and MWCNT, considerable enhancement in thermal and mechanical properties was achieved in the composites. With addition of just 0.5 wt% Mt – MWCNT (Mt:MWCNTs = 10:1, w/w), the tensile strength and modulus of epoxy-based composites were improved by 42.0% and 20.3%, respectively, compared with pure epoxy. Furthermore, the storage modulus in the glassy region increased by 21.2%. Moreover, the glass-transition and onset decomposition temperatures were also significantly enhanced, implying the superior thermal stability of these composites.

1. Introduction

Epoxy resin (EP) is widely used in engineering applications due to its inherent advantages such as excellent dimensional stability, resistance to heat and chemicals, easy-processability and low-cost [1]. However, most cured epoxies are generally brittle and exhibit poor resistance to crack initiation and propagation, which largely hinder its application [2]. To improve the toughness of the cured EP, the composite strategy has been used which involves the use of additives, such as rubbers [3], thermoplastics [4], and organic or inorganic nanoparticles [5].

Among the various additives, one-dimensional (1D) carbon nanotubes (CNTs) are particularly attractive due to their high strength and modulus, low density and large aspect ratios [6–8]. On the other hand, two-dimensional (2D) montmorillonite (Mt) has also garnered interest because of its large surface area, strong adsorption ability and ion-exchange property [9,10]. Incorporating a small amount of CNTs or Mt into EP can provide enhancements in both mechanical and thermal properties of the resulting composites [11,12].

Recently, introducing a combination of CNTs and Mt into polymers for constructing hybrid composites has been demonstrated to be an alternative strategy for further enhancing the properties of polymers due to the synergistic effect [13]. Based on the fact that the final performance of composites largely depends on the nanofillers dispersion, it is essential to achieve good dispersion of hybrids in the matrix to exert their maximum benefits. To date, the most common method to produce hybrid composites is to simply disperse CNTs and Mt separately in a liquid resin with the aid of sonication, high-speed stirring, or three-roll milling [14,15]. However, this method is only applicable for low loadings due to the easy re-agglomeration of CNTs in resin at high loadings [16]. Moreover, the exfoliation of Mt in matrices still remains a challenge even though Mt is organically modified. Several techniques such as chemical vapor deposition (CVD) [17], dry grinding [18], and chemical modification [19] have been applied to improve the dispersion ability of CNTs and Mt in matrix. For example, CNTs can be directly grown on Mt layers by CVD, forming a nanostructured hybrid and thus improving the dispersion level of CNTs and Mt in polymeric matrix [20]. However, it should be noted that these techniques are always costly/tedious and not suitable for large-scale production. Thus, exploring an effective method to achieve uniform dispersions of CNTs and Mt simultaneously with high loadings is an ongoing task.

Herein, a simple yet effective self-assembly method was designed to prepare Mt – MWCNT hybrids to improve the dispersion ability of hybrids in epoxy matrix. Using carboxyl MWCNTs and Mt as starting materials, a nanostructured hybrid was obtained through a cation exchange reaction, in which different amounts of MWCNTs were attached on the exfoliated Mt. Based on hybrid design, the structural performance of MWCNTs and Mt can be maximized and benefit from possible synergistic effects. The obtained results showed that the composites containing Mt – MWCNT presented superior mechanical and thermal

* Corresponding author.
E-mail address: mxshen@hhu.edu.cn (M. Shen).

https://doi.org/10.1016/j.compscitech.2018.04.035
Received 24 February 2018; Received in revised form 21 April 2018; Accepted 26 April 2018
Available online 27 April 2018

properties, compared with the composites filled with individual MWCNTs and Mt. Moreover, by employing this self-assembly method, one can tailor the MWCNTs content in hybrids and subsequently tune the mechanical and thermal properties of epoxy-based composites. This study demonstrates a practical and scalable strategy to optimize the mechanical and thermal properties of epoxy-based composites using a nanostructured hybrid, thus offering a novel strategy to design epoxy-based composites for practical applications requiring high performance.

2. Experimental

2.1. Materials

Industrial-grade carboxyl MWCNTs (carbon: ≥90%, diameter: 20–40 nm, length: ~30 μm, −COOH content: ~1.43 wt%) were provided by Chengdu Organic Chemicals Co., Ltd. (Chengdu, China). Mt (FH−F3w; purity: ≥95%) with a cation exchange capacity of ~110 mmol/100 g was supplied by Zhenjiang Fenghong New Material Co., Ltd (Huzhou, China). Bisphenol-A type epoxy resin (Araldite LY 1564 SP; viscosity: 1200–1400 mPa s) and its amine hardener (Aradur 3486; viscosity: 10–20 mPa s) were received from Huntsman Advanced Materials Americas Inc. (Woodlands, Texas, USA). The other chemicals including concentrated hydrochloric acid (HCl), dimethylformamide (DMF), diisopropylcarbodiimide (DIC), 1-hydroxybenzotriazole (HOBt) and triethylenetetramine (TETA) were purchased from Nanjing Chemical Reagent Co., Ltd (Nanjing, China).

2.2. Synthesis of self-assembled Mt–MWCNT

The preparation procedure of self-assembled Mt–MWCNT is as follows (see Fig. 1 (Stage 1)):

(1) First, 2 mg DIC and 2 mg HOBt were dissolved in 30 mL DMF. Then, 100 mg of carboxyl MWCNTs was dispersed into the above solution using an ultrasonic bath operated at 600 W for 0.5 h. Subsequently, 50 mg TETA was added into the MWCNTs suspension dropwise with stirring, followed by stirring magnetically at room temperature for 24 h. The precipitate was filtered through a polycarbonate membrane (0.2 μm pore size) and washed three times with deionized water, to obtain the amine-functionalized MWCNTs [21,22].
(2) The amine-functionalized MWCNTs were dispersed in 30 mL deionized water with ultrasonication, and 2 mL concentrated HCl was added dropwise with stirring. After stirring for 0.5 h, the ammonium salts-grafted MWCNTs were obtained.
(3) 1000 mg Mt was dispersed in 40 mL deionized water with ultrasonication and then heated to 80 °C for 0.5 h. The above ammonium salts-grafted MWCNTs were added and stirred together overnight at 80 °C. Finally, the filtrate was washed three times with deionized water and then dried under vacuum at 90 °C overnight to obtain the self-assembled Mt–MWCNT. Herein, the weight ratio of Mt to MWCNTs was 1:10.

2.3. Fabrication of epoxy composites

The epoxy composites containing Mt − MWCNT were fabricated by a solution intercalation method, as shown in Fig. 1 (Stage 2). The obtained Mt − MWCNT nanofillers were dispersed in epoxy resins by stirring magnetically at 400 rpm for 24 h and then ultrasonicating for 0.5 h. To further improve the dispersion and exfoliation of Mt − MWCNT nanofillers in resins, the mixture was subsequently passed

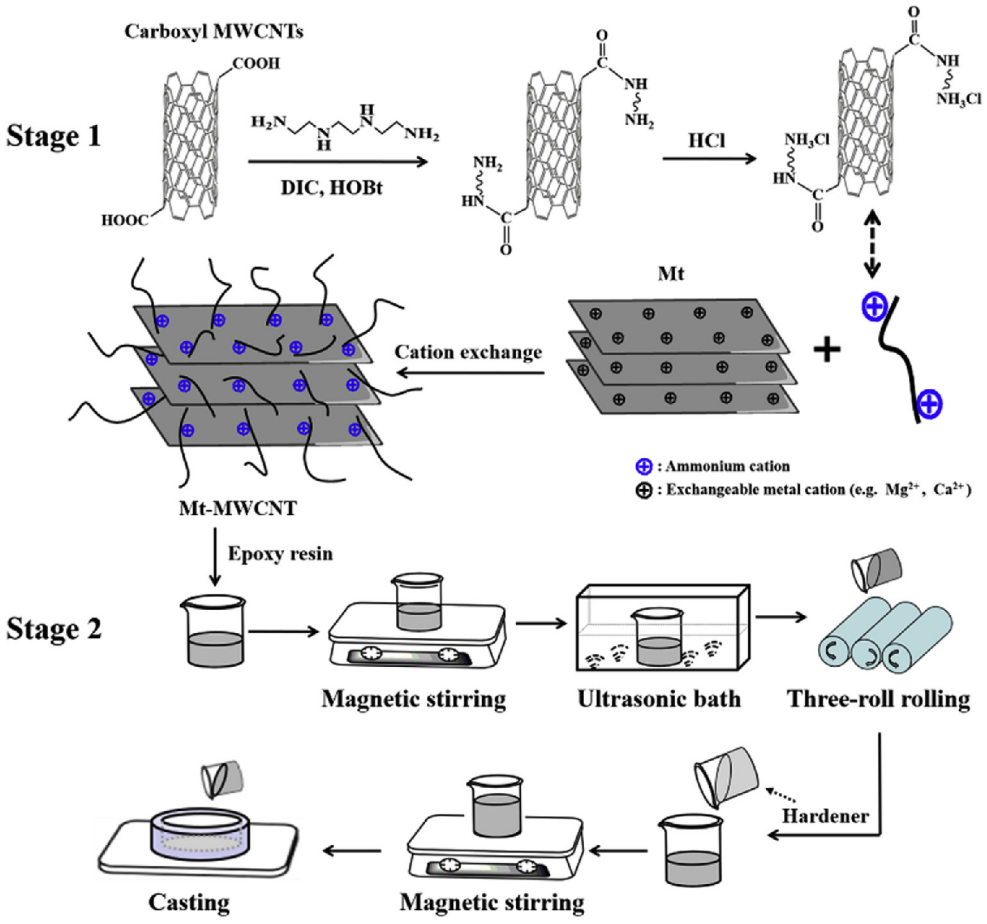

Fig. 1. Schematic of preparation of (Stage 1) self-assembled Mt–MWCNT and (Stage 2) its composites.

through a three-roll grinder (Exakt 50; EXAKT GmbH, Norderstedt, Germany). A varying gap was set between feeding roller and center roller, and three passes of 20 μm (1st pass), 10 μm (2nd pass) and 5 μm (3rd pass) were used to induce high shear force for the mixture. For the three passes, the speed of three rollers was maintained at a ratio of 1:1.8:3.3 with a maximum speed of 200 rpm.

After the three-roll rolling process, the amine hardener was added into the above mixture with epoxy:hardener weight ratio of 100:34 and the mixture was magnetically stirred for 10 min at 600 rpm. The Mt − MWCNT/resin suspensions were degassed under vacuum at 40 °C for 15 min, and then cast in polytetrafluoroethylene molds. The specimens were first cured at room temperature for 24 h, followed by post-curing treatment at 80 °C for 8 h.

The epoxy composites containing 0.1 wt%, 0.3 wt%, 0.5 wt% and 0.7 wt% of Mt–MWCNT were obtained and labeled as E/MM-0.1, E/MM-0.3, E/MM-0.5 and E/MM-0.7, respectively. For the sake of comparison, the epoxy composites containing 0.5 wt% MWCNTs and Mt were individually prepared using similar procedures, and labeled as E/MWCNT-0.5 and E/Mt-0.5, respectively. Herein, pristine Mt was also treated by the same ultrasonic and thermal conditions as Mt–MWCNT prior to composite fabrication.

2.4. Characterization

Fourier transform infrared spectroscopy (FTIR; Vertex 80v, Bruker, Germany) was employed to record the wave numbers of the samples from 400 to 4000 cm^{-1}. The surface morphology of nanofillers and cross-sectional morphology of composites were investigated by field emission scanning electron microscopy (SEM; SU8010, Hitachi, Japan). The element analysis of interface regions between MWCNTs and Mt was performed on an energy dispersive X-ray spectrometer (EDX; EX-250, Horiba, Japan). All the observed specimens were plated.

The microstructure of nanofillers and their distribution in the composite was characterized by transmission electron microscopy (TEM; JEM-1400, JEOL, Japan) operated at 200 kV. The structural changes of nanofillers and their composites were investigated by X-ray diffraction (XRD, ARL-X'TRA, Thermo Scientific, USA) at room temperature with Cu-target Kα radiation (λ = 0.154 nm).

The tensile test referred to ISO 527-2:2012 was performed on a universal testing machine (Model 3343, Instron Corp., Canton, Mass., USA) at room temperature. Each effective datum was the average of five specimens. Dynamic mechanical thermal analysis (DMTA) was examined using a dynamic thermo-mechanical analyzer (Q800, TA instruments, USA) operating in the three-point bending mode at a constant frequency of 1 Hz under air. The effective data were recorded from room temperature to 180 °C at a heating rate of 5 °C/min. Thermal gravimetric analysis (TGA) was carried out on a thermal analyzer (STA409/PC, NETZSCH, Germany) heating from room temperature to 800 °C under nitrogen atmosphere at a heating rate of 10 °C/min.

3. Results and discussion

3.1. Structure and morphology of Mt–MWCNT

The structures of Mt, carboxyl MWCNTs and Mt–MWCNT were investigated by XRD analysis, and the results are plotted in Fig. 2(a). For the pristine Mt, a sharp diffraction peak at about 7.07° is observed, which is attributed to the 001 reflection, corresponding to the d_{001} spacing of 1.25 nm. In the case of Mt–MWCNT, the 001 reflection of Mt is shifted to 4.19°, indicating that the d_{001} spacing is expanded by about 0.86 nm. This suggests that the layered Mt is pre-exfoliated by the TETA molecules attached on the MWCNTs [23]. The exfoliation of Mt induced by TETA salt-modified MWCNTs is also clearly seen in the TEM image (Fig. 2(b)), where a single Mt sheet surrounded by MWCNTs is observed while overlapped layered structures are present in pristine Mt.

To evaluate the interaction between Mt and MWCNTs, FTIR measurement was performed, as presented in Fig. 3(a). For the Mt, the peak at 3632 cm^{-1} is assigned to the O−H stretching of lattice water in Mt, and the stretching and deformation bands of −OH on Mt layers are observed at 3436 and 1640 cm^{-1} [24]. The peaks at 1031 and 463 cm^{-1} are ascribed to the stretching and bending vibrations of Si−O. All of the above peaks are observed for both Mt and Mt − MWCNT. In the spectrum of carboxyl MWCNTs, the peak at 1705 cm^{-1} is a typical absorption of the carbonyl group (C═O) [25], arising from −COOH moieties on carboxyl MWCNTs. It should be noted that the peak intensity at 3436 cm^{-1} of Mt − MWCNT is greater than that of carboxyl MWCNTs, which is presumably due to the overlapping absorption of stretching vibrations of −OH and −NH−. The weak peak at 1157 cm^{-1} is assigned to the bending vibration of C−N. The peaks at 2931, 2853 and 1463 cm^{-1} are related to the stretching and bending vibrations of $-CH_2-$, which comes from the TETA salts. Therefore, the presence of $-CH_2-$, −NH− and C−N demonstrates that TETA salts are successfully attached on the surface of MWCNTs via covalent bonds.

The interaction between Mt and MWCNTs was also elucidated by SEM and EDX, as shown in Fig. 3(b). The elements Mg and Ca come from the exchangeable metal ions that exist in Mt. The element C is from the additives in Mt or carboxyl MWCNTs or TETA, and element N is mainly from TETA. With the addition of TETA salts-modified MWCNTs, the C% of Mt − MWCNT is improved by about 1.7 times. Moreover, element N appears and its content is increased to 13.38%, while the total amount of Mg and Ca decline sharply from 23.48% to 2.22%, compared with original Mt. These results indicate that a good connection is achieved between Mt and MWCNTs via a cation-exchange reaction.

From the above results, it can be concluded that TETA salt-modified MWCNTs are beneficial to pre-exfoliate Mt and establish a strong interfacial bond with Mt.

3.2. Structure of composites

TEM was performed to analyze the dispersion of Mt–MWCNT in epoxy composites, and the images are shown in Fig. 4. For the sake of comparison, TEM images for the dispersions of pristine Mt and carboxyl MWCNTs are also given. As seen, pristine Mt still maintains the stacking state in the E/Mt-0.5. For the E/MWCNT-0.5, most of the MWCNTs are dispersed well in the composite while some small MWCNTs agglomerates are still observed. For the composite containing Mt − MWCNT (E/MM-0.5), well-dispersed MWCNTs and exfoliated Mt are observed. Moreover, it is clear that MWCNTs are interlocked with the layers of Mt. These results indicate that the presence of Mt nanosheets prevents the re-agglomeration of MWCNTs, while the MWCNTs facilitate the dispersion and exfoliation of Mt in the composites.

The structural phase of epoxy composites containing Mt, carboxyl MWCNTs, and Mt–MWCNT was analyzed by XRD, as shown in Fig. 5. Pure EP exhibits a broad peak at 17.8°, which is attributed to the amorphous nature of EP [26]. In case of E/Mt-0.5, the characteristic peak of Mt appears at 6.1°, owing to the stacking of Mt in matrix. It should be noted that the characteristic peak of Mt is absent in epoxy composites containing Mt–MWCNT, indicating the exfoliation of Mt in matrix. Furthermore, the stronger intensity of the peak at 17.8° can be explained by the increased Mt–MWCNT contents.

3.3. Mechanical properties of composites

The tensile properties of epoxy composites containing Mt, MWCNTs and Mt–MWCNT are shown in Fig. 6(a) and (b). It is evident that the tensile properties of E/MM-0.5 are stronger than those of E/Mt-0.5 and E/MWCNT-0.5. Compared with pure EP, the tensile strength and Young's modulus of E/MM-0.5 are improved by 42.0% and 20.3% (Fig. 6(a)), respectively. Also, the elongation at break of E/MM-0.5 is higher than that of E/Mt-0.5 and E/MWCNT-0.5 (Fig. 6(b)), indicating the ductile fracture for epoxy composites containing Mt–MWCNT.

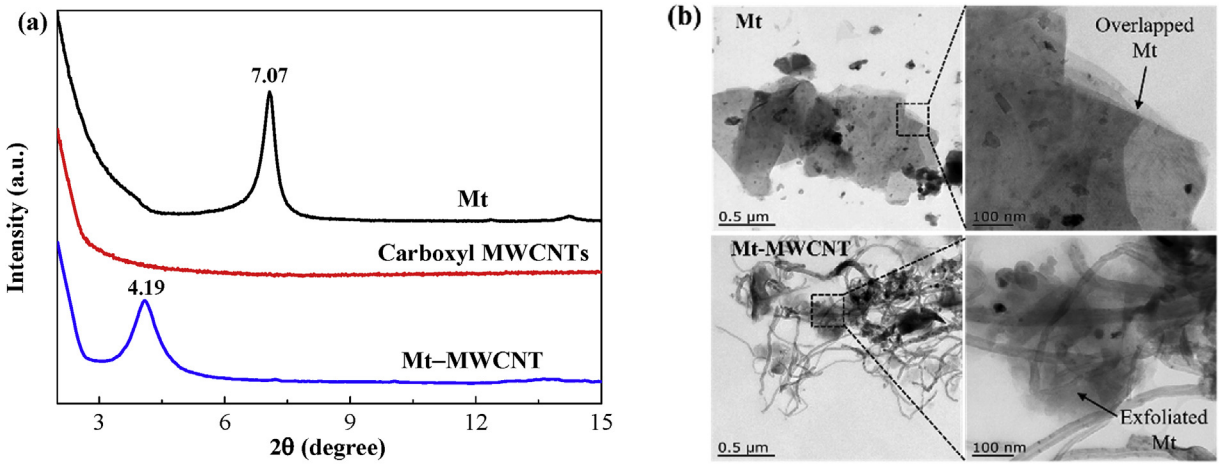

Fig. 2. (a) XRD patterns of Mt, carboxyl MWCNTs and Mt − MWCNT; (b) TEM images of Mt and Mt − MWCNT at two different magnifications.

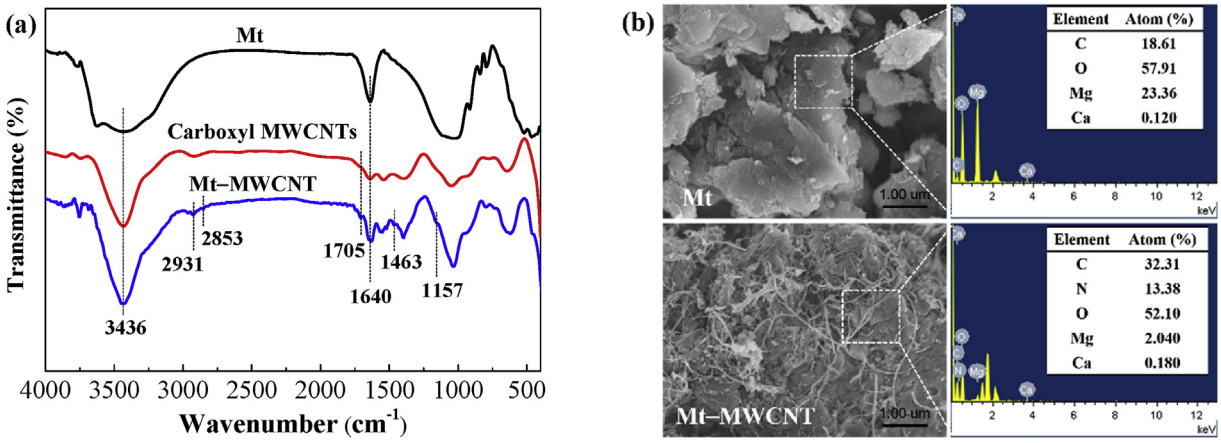

Fig. 3. (a) FTIR spectra of Mt, carboxyl MWCNTs and Mt − MWCNT; (b) SEM images and EDX spectrums of Mt and Mt–MWCNT.

These results indicate that the synergistic effect of MWCNTs and Mt is advantageous for the improvement in mechanical properties of the composites.

Furthermore, tensile properties of epoxy composites containing various Mt–MWCNT contents were also evaluated, as presented in Fig. 6(c) and (d). With increase in Mt–MWCNT contents, both tensile strength and Young's modulus of epoxy composites increase at first and then begin to decline as the Mt–MWCNT content reaches to 0.5 wt%. The lower tensile strength and Young's modulus of epoxy composites filled with 0.7 wt% Mt–MWCNT are likely due to the inevitable aggregation of nanosheets under high Mt–MWCNT contents. Additionally, the maximum improvement of elongation at break (39.7%) is obtained when 0.3 wt% of Mt–MWCNT is incorporated.

These considerable improvements in tensile properties are attributed to the homogeneous dispersion of Mt–MWCNT in matrix and strong interfacial interactions between Mt–MWCNT and matrix. This is supported by the SEM observations shown in Fig. 7. From the cross-sectional SEM image of the composites filled with pristine Mt, displayed

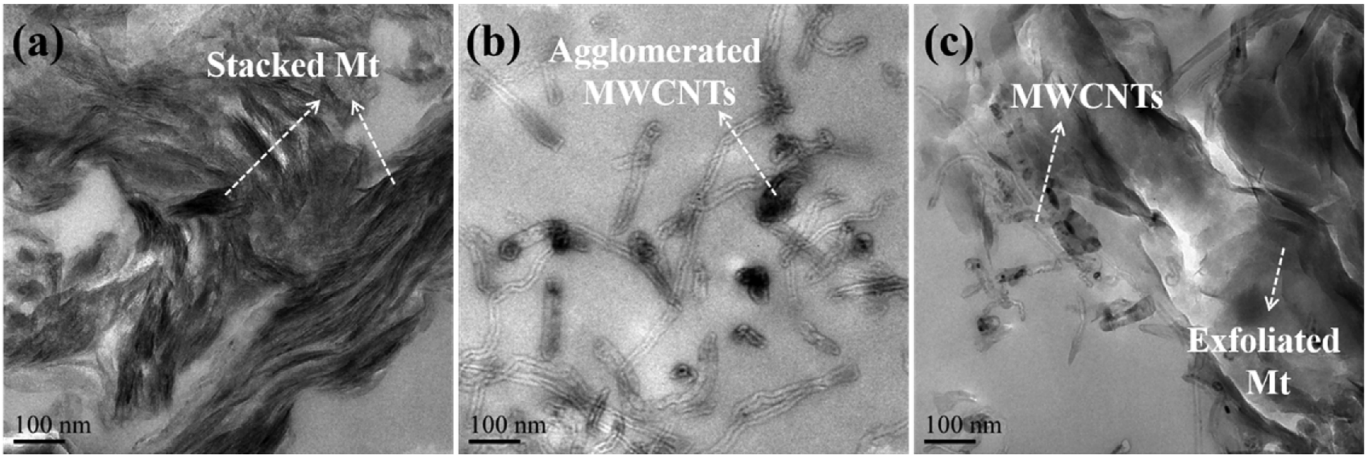

Fig. 4. TEM images of epoxy composites: (a) E/Mt-0.5, (b) E/MWCNT-0.5 and (c) E/MM-0.5.

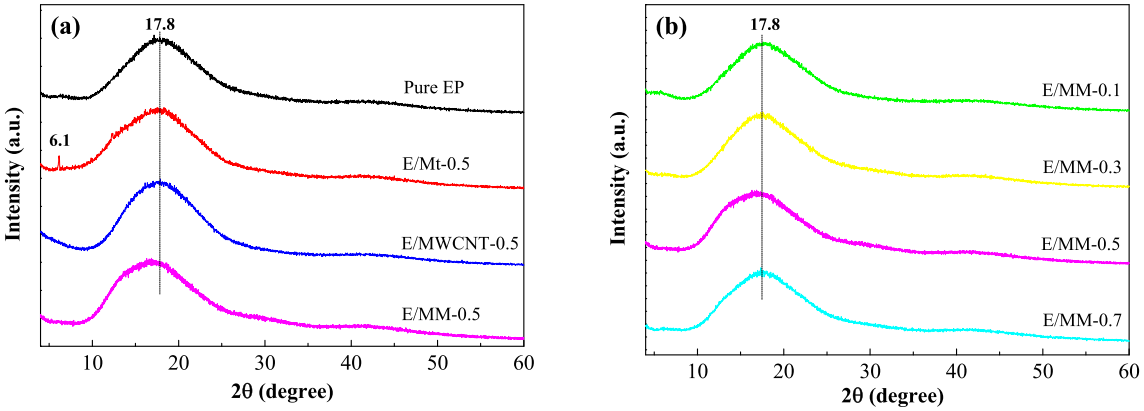

Fig. 5. XRD patterns of epoxy composites containing (a) different nanofillers and (b) various Mt–MWCNT contents.

in Fig. 7(a), it is clear that the cracks end in the stacked Mt, indicating the interface debonding behavior and poor interfacial bonding between Mt and matrix. In Fig. 7(b) and (c), pulled-out MWCNTs and bridged MWCNTs are evident, indicating that more energy is absorbed in matrix deformation and crack propagation. Moreover, both MWCNTs and Mt can act as crack arresters to prevent the expansion of micro-cracks. It is believed that the MWCNTs anchored on the surface of Mt nanosheets provide mechanical interlocking at the Mt/matrix interface and thus improve the interfacial interaction. As seen in Fig. 7(d), the matrix is tightly attached to the surface of MWCNTs, indicating the strong interfacial adhesion caused by covalent interactions between the amino groups of Mt-MWCNT and epoxy [27,28].

It should be mentioned here that the 1D/2D structural network consisting of the MWCNTs and Mt, can facilitate the stress transfer from matrix phase to nanofillers and prevent the initiation and propagation of cracks. Moreover, several toughening mechanisms simultaneously contribute the fracture toughness, including MWCNTs bridging, MWCNT pull-out and crack deflection and pinning [29]. From Fig. 8, it is evident that the surface roughness of epoxy composites containing Mt–MWCNT is greater than that of pure EP. Furthermore, the fracture surface of epoxy composites containing Mt–MWCNT has a tendency to become rougher with the increase in Mt–MWCNT contents. However, the brittle fracture surface is also found in E/MM-0.7 (Fig. 8(e)), probably due to the Mt–MWCNT agglomerates. Therefore, good

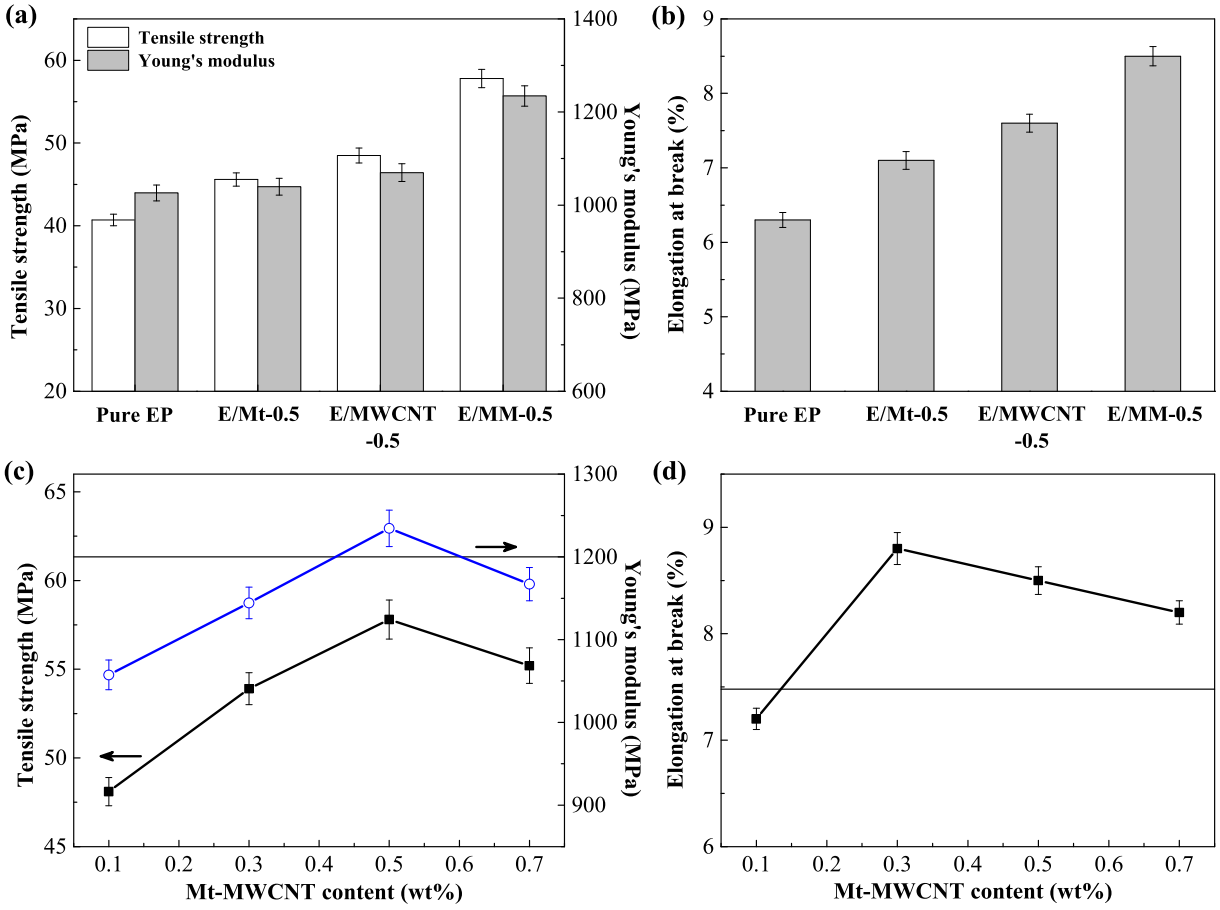

Fig. 6. Tensile strength, Young's modulus and elongation at break of epoxy composites containing (a, b) different nanofillers and (c, d) various Mt–MWCNT contents, respectively.

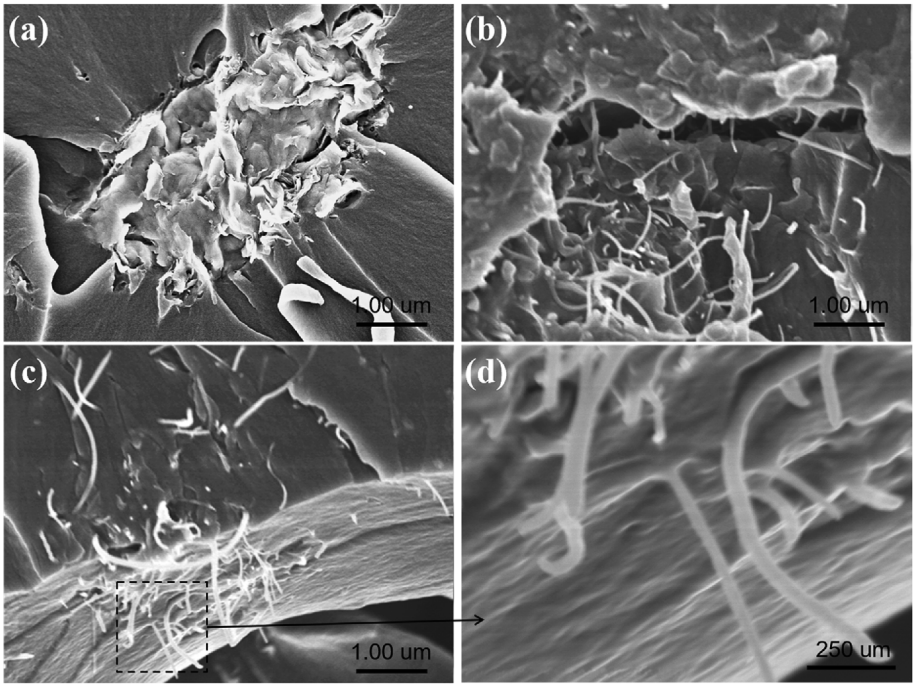

Fig. 7. SEM images showing the interfacial adhesion of epoxy composites: (a) E/Mt-0.5, (b) E/MWCNT-0.5, and (c), (d) E/MM-0.5.

dispersion of Mt–MWCNT in matrix and strong interfacial adhesion between Mt-MWCNT and epoxy matrix can increase energy dissipation during the matrix deformation and delay material failure.

3.4. Dynamic mechanical thermal properties of composites

DMTA was preformed to investigate the viscoelastic behavior of polymer composites. Fig. 9 shows the curves of storage modulus (E') and loss factor (tan δ) as a function of temperature. The values of E' in the glassy region at 30 °C (E'_{30}), glass-transition temperature (T_g), and height of loss factor (tan δ_{max}) for the composites are listed in Table 1.

Fig. 9(a) and (b) show the E' of epoxy composites containing different nanofillers and various Mt–MWCNT contents, respectively. As observed in Fig. 9(a), the E' values of epoxy composites in the glassy region are increased due to the addition of nanofillers. Moreover, the E' of E/MM-0.5 is much higher than that of E/Mt-0.5 and E/MWCNT-0.5. The maximum increment (21.2%) in E'_{30} value relative to pure EP is obtained for E/MM-0.5. Such a significant improvement in E' can be attributed to the synergistic reinforcement of Mt and MWCNTs, significantly improved interfacial interaction, and the mobility restriction of epoxy molecules. Furthermore, it is noted that the E' is improved with increasing Mt–MWCNT contents, as seen in Fig. 9(b). However, a

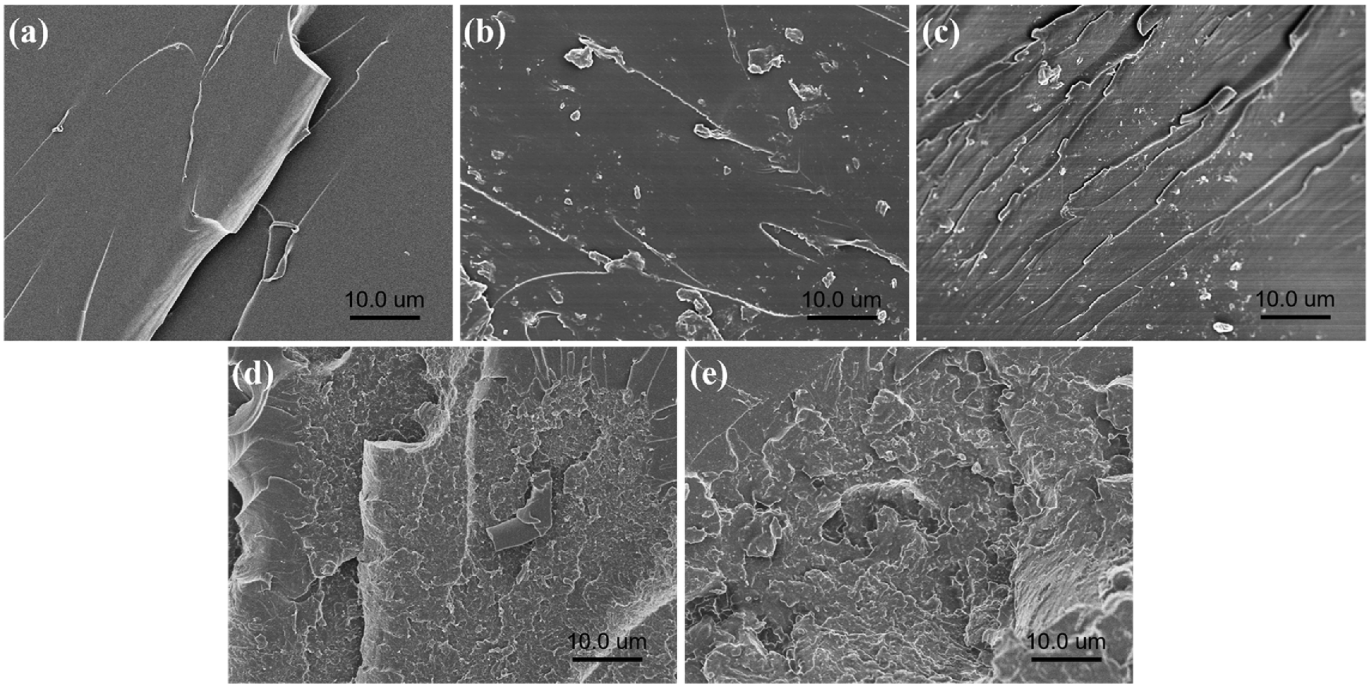

Fig. 8. SEM images of fracture surface of tensile specimens: (a) Pure EP, (b) E/MM-0.1, (c) E/MM-0.3, (d) E/MM-0.5 and (e) E/MM-0.7.

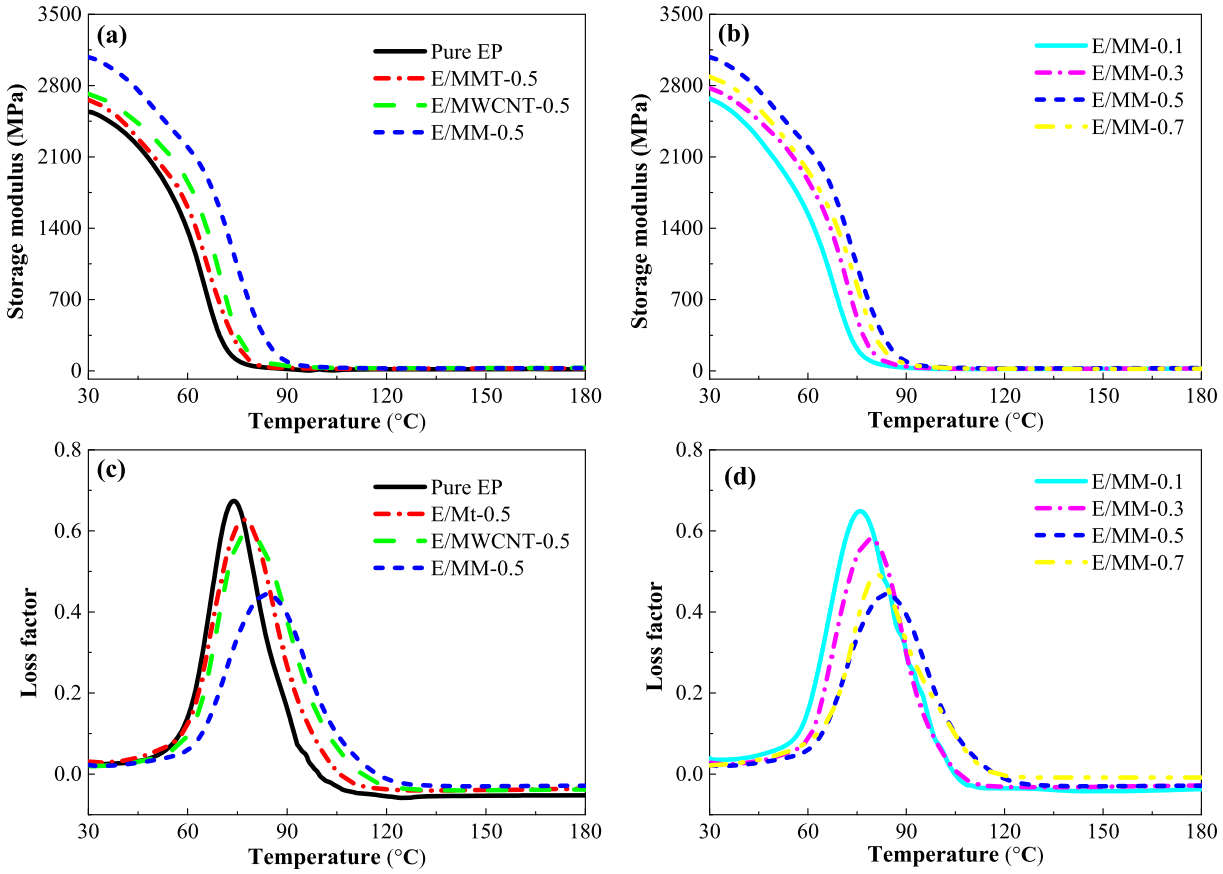

Fig. 9. Storage modulus (a, b) and loss factor (c, d) vs. temperature curves of epoxy composites containing different nanofillers and various Mt–MWCNT contents, respectively.

Table 1
The DMTA and TGA results of epoxy composites.

Sample	DMTA			TGA		
	E'_{30} (MPa)	T_g (°C)	Tan δ_{max}	T_5 (°C)	T_{50} (°C)	Residue at 800 °C (wt. %)
Pure EP	2540	73.82	0.6742	355.7	385.4	7.685
E/Mt-0.5	2658	76.99	0.6275	357.9	388.8	8.350
E/MWCNT-0.5	2719	78.06	0.5948	361.4	393.4	8.656
E/MM-0.1	2672	75.88	0.6488	359.7	390.8	8.423
E/MM-0.3	2775	79.07	0.5792	362.6	396.5	9.295
E/MM-0.5	3078	83.97	0.4437	371.0	403.6	10.66
E/MM-0.7	2887	81.00	0.4925	366.4	399.5	8.867

slight decrease in E' is observed when the Mt–MWCNT content is increased to 0.7 wt%. This behavior is probably due to the incomplete impregnation of Mt–MWCNT agglomerates by epoxy resin, which results in reduced interfacial interactions.

As shown in Fig. 9(c), there is a height reduction of tan δ as well as shifting of tan δ peak temperature (i.e. T_g) in epoxy composites. The maximum decrement in tan δ_{max} (0.2305) and maximum increment in T_g (10.2 °C) are observed for E/MM-0.5, as compared with pure EP. From Fig. 10(d), the T_g of epoxy composites is initially enhanced with the increase in Mt–MWCNT content. The T_g decreases when the Mt–MWCNT content reaches to 0.7 wt%. The decrease in tan δ indicates the lower mechanical loss in epoxy composites. Mt–MWCNT networks are more effective for restricting the movement of epoxy molecules in composites, resulting in a higher T_g. Moreover, the uniform dispersion of Mt–MWCNT and strong interfacial interaction between Mt-MWCNT and epoxy matrix can further facilitate the positive shift of T_g. In contrast, Mt–MWCNT agglomerates may cause the formation of free volume in matrix and thus facilitate the motion of epoxy molecules, which leads to a drop in T_g.

3.5. Thermal properties of composites

TGA can reveal the thermal properties and the decomposition process of polymer composites. Fig. 10 shows the TGA curves of epoxy composites containing different nanofillers and various Mt–MWCNT contents. The corresponding decomposition temperatures at 5% weight loss (T_5) and 50% weight loss (T_{50}) and char residue at 800 °C are provided in Table 1.

As shown in Fig. 10(a), both T_5 and T_{50} of epoxy composites are higher than those of pure EP, following an order of E/MM-0.5 > E/MWCNT-0.5 > E/Mt-0.5. Compared with pure EP, the T_5 and T_{50} of E/MM-0.5 are increased by 15.3 °C and 18.3 °C, respectively. The total residue of epoxy composites at 800 °C is increased by about 0.7–3.0% (Table 1). The highest amount of char residue is observed for E/MM-0.5. These results indicate that the thermal stability of epoxy composites containing Mt–MWCNT is much superior to that of pure EP or the composite individually filled by MWCNT or Mt. This enhanced thermal stability can be attributed to the barrier effect of Mt–MWCNT. Mt acts as an energy storage medium to hinder thermal transfer within the matrix. The MWCNTs inlaid between the Mt nanosheets can facilitate the formation of thermally stable carbonaceous char, which serves as a heat barrier or thermal insulation to reduce the decomposition of epoxy matrices [30].

As seen in Fig. 10(b), with increase in Mt–MWCNT contents, both T_5 and T_{50} of epoxy composites containing Mt–MWCNT increase at first and then begin to decline as the Mt–MWCNT content reaches to 0.5 wt % (Table 1). This is attributed to the uniform dispersion of Mt–MWCNT

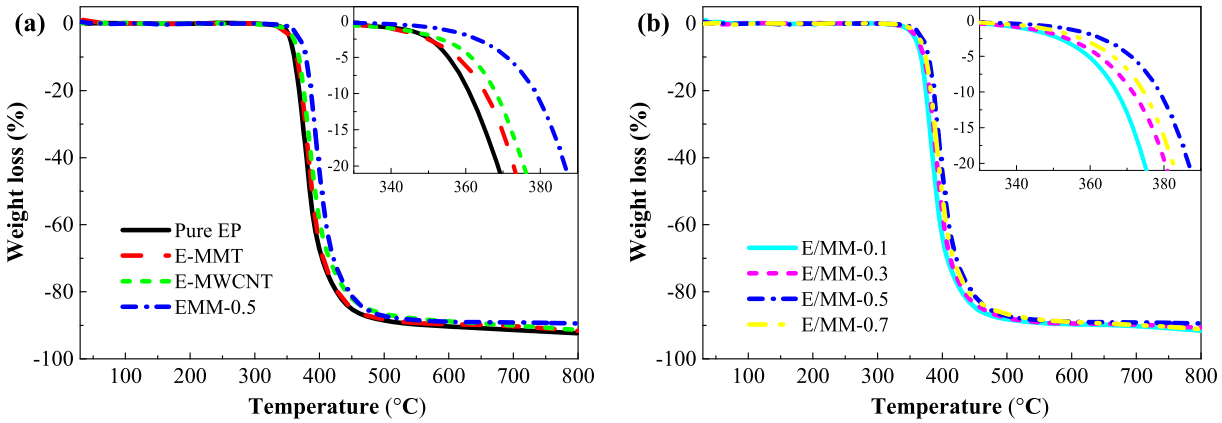

Fig. 10. TGA curves of epoxy composites containing (a) different nanofillers and (b) various Mt–MWCNT contents.

and the strong interfacial interaction between Mt–MWCNT and matrix. The decrease in thermal stability at higher loadings is probably caused by the re-aggregation of Mt–MWCNT in matrix.

4. Conclusions

In this work, a nanostructured hybrid consisting of montmorillonite–multi-walled carbon nanotube (Mt–MWCNT) was designed and prepared using a novel, effective self-assembly method. A strong interaction between Mt and MWCNTs could be achieved via covalent bonding and cation exchange reaction. Subsequently, three-roll milling combined with ultrasonic dispersion technique was utilized to disperse Mt–MWCNT hybrids in epoxy resins. The obtained epoxy composites exhibited superior mechanical and thermal properties compared to the composites filled with individual MWCNTs and Mt. The main findings of this work are as follows.

1. Triethylenetetramine salts grafted on the surface of MWCNTs assisted in the pre-exfoliation of Mt and ultimately led to the formation of a completely exfoliated structure in matrix. In addition, the dispersion state of MWCNTs could be improved due to the barrier effect of Mt nanosheets.
2. Due to the synergistic effect of Mt and MWCNTs, the self-assembled Mt–MWCNT exhibited higher efficiency in reinforcing epoxy composites. MWCNTs anchored on the surface of Mt nanosheets provided mechanical interlocking to improve interfacial interaction and facilitate the stress transfer. Furthermore, Mt acted as an energy storage medium to resist micro-crack extension and hinder thermal transfer within the matrix.
3. The optimized Mt–MWCNT loading was found to be 0.5 wt%, where the mechanical and thermal properties of epoxy composites reached the peak values. With an addition of 0.5 wt% Mt–MWCNT, the tensile strength and modulus of epoxy composites increased by 42.0% and 20.3%, respectively; the storage modulus in the glassy region was improved by 21.2%; and the glass-transition and thermal decomposition temperatures were significantly increased. In addition, the elongation at break had a maximum increment of 39.7% at 0.3 wt% of Mt–MWCNT loading.

Acknowledgments

This work was supported by the Fundamental Research Funds for the Central Universities, China (grant number 2018B40814).

Appendix A. Supplementary data

Supplementary data related to this article can be found at http://dx.doi.org/10.1016/j.compscitech.2018.04.035.

References

[1] S. Sprenger, Epoxy resin composites with surface-modified silicon dioxide nanoparticles: a review, J. Appl. Polym. Sci. 130 (2013) 1421–1428.
[2] A.H. Korayem, M.R. Barati, G.P. Simon, X.L. Zhao, W.H. Duan, Reinforcing brittle and ductile epoxy matrices using carbon nanotubes masterbatch, Compos. Appl. Sci. Manuf. 61 (2014) 126–133.
[3] D. Carolan, A. Ivankovic, A.J. Kinloch, S. Sprenger, A.C. Taylor, Toughening of epoxy-based hybrid nanocomposites, Polymer 97 (2016) 179–190.
[4] J.H. Hodgkin, G.P. Simon, R.J. Varley, Thermoplastic toughening of epoxy resins: a critical review, Polym. Adv. Technol. 9 (2015) 3–10.
[5] Yong Ni, S. Zheng, Nanostructured thermosets from epoxy resin and an Organic－Inorganic amphiphile, Macromolecules 40 (2007) 7009–7018.
[6] L. Yang, H. Ji, K. Zhu, J. Wang, J. Qiu, Dramatically improved piezoelectric properties of poly(vinylidene fluoride) composites by incorporating aligned TiO 2 @MWCNTs, Compos. Sci. Technol. 123 (2016) 259–267.
[7] C.Q. Li, J.W. Zha, Z.J. Li, D.L. Zhang, S.J. Wang, Z.M. Dang, Towards balanced mechanical and electrical properties of thermoplastic vulcanizates composites via unique synergistic effects of single-walled carbon nanotubes and graphene, Compos. Sci. Technol. 157 (2018) 134–143.
[8] S. Zeng, M. Shen, P. Duan, Y. Xue, Z. Wang, Effect of silane hydrolysis on the interfacial adhesion of carbon nanotubes/glass fiber fabric-reinforced multiscale composites, Textil. Res. J. 88 (2018) 379–391.
[9] M.X. Shen, P.P. Duan, Y.Q. Han, Effect of montmorillonite on moisture resistance of the rubber-modified phenolic on fiberglass, J. Compos. Mater. 48 (2014) 1347–1353.
[10] Y.T. Tsai, J.Y. Chiou, C.Y. Liao, P.Y. Chen, S.H. Tung, J.J. Lin, Organically modified clays as rheology modifiers and dispersing agents for epoxy packing of white LED, Compos. Sci. Technol. 132 (2016) 9–15.
[11] A. Tcherbi-Narteh, M. Hosur, E. Triggs, P. Owuor, S. Jelaani, Viscoelastic and thermal properties of full and partially cured DGEBA epoxy resin composites modified with montmorillonite nanoclay exposed to UV radiation, Polym. Degrad. Stabil. 101 (2014) 81–91.
[12] I.D. Rosca, S.V. Hoa, Method for reducing contact resistivity of carbon nanotube-containing epoxy adhesives for aerospace applications, Compos. Sci. Technol. 71 (2011) 95–100.
[13] M.H. Al-Saleh, Clay/carbon nanotube hybrid mixture to reduce the electrical percolation threshold of polymer nanocomposites, Compos. Sci. Technol. 149 (2017) 34–40.
[14] P. Pötschke, B. Krause, S.T. Buschhorn, U. Köpke, M.T. Müller, T. Villmow, K. Schulte, Improvement of carbon nanotube dispersion in thermoplastic composites using a three roll mill at elevated temperatures, Compos. Sci. Technol. 74 (2013) 78–84.
[15] M.M. Rahman, S. Zainuddin, M.V. Hosur, J.E. Malone, M. Salam, A. Kumar, S. Jeelani, Improvements in mechanical and thermo-mechanical properties of e-glass/epoxy composites using amino functionalized MWCNTs, Compos. Struct. 94 (2012) 2397–2406.
[16] P.C. Ma, S.Y. Mo, B.Z. Tang, J.K. Kim, Dispersion, interfacial interaction and re-agglomeration of functionalized carbon nanotubes in epoxy composites, Carbon 48 (2010) 1824–1834.
[17] E. Esmizadeh, A.A. Yousefi, G. Naderi, C. Milone, Drastic increase in catalyst productivity of nanoclay-supported CVD-grown carbon nanotubes by organo-modification, Appl. Clay Sci. 118 (2015) 248–257.
[18] B. Pradhan, S. Roy, S.K. Srivastava, A. Saxena, Synergistic effect of carbon nanotubes and clay platelets in reinforcing properties of silicone rubber nanocomposites, J. Appl. Polym. Sci. 132 (2015) 871–882.
[19] S. Zhao, C. Li, Y. Zhou, S. Wang, F. Su, J. Cui, Y. Yan, A multifunctional hydrogel based on heterostructured hybrids of single-walled carbon nanotubes and clay nanoplatelets, Carbon 77 (2014) 846–856.
[20] L. Madaleno, R. Pyrz, A. Crosky, L.R. Jensen, J.C.M. Rauhe, V. Dolomanova, J.J.C. Pinto, J. Norman, Processing and characterization of polyurethane nanocomposite foam reinforced with montmorillonite–carbon nanotube hybrids,

Compos. Appl. Sci. Manuf. 44 (2013) 1–7.
[21] M.-L. Sham, J.-K. Kim, Surface functionalities of multi-wall carbon nanotubes after UV/Ozone and TETA treatments, Carbon 44 (2006) 768–777.
[22] Z.A. Alothman, E. Yilmaz, M.A. Habila, I.H. Alsohaimi, A.M. Aldawsari, N.M. Alharbi, M. Soylak, Triethylenetetramine modified multiwalled carbon nanotubes for the efficient preconcentration of Pb(II), Cu(II), Ni(II) and Cd(II) before FAAS detection, RSC Adv. 5 (2015) 106905–106911.
[23] B. Gong, P. Wu, Z. Huang, Y. Li, S. Yang, Z. Dang, B. Ruan, C. Kang, Efficient inhibition of heavy metal release from mine tailings against acid rain exposure by triethylenetetramine intercalated montmorillonite (TETA-Mt), J. Hazard Mater. 318 (2016) 396–406.
[24] Y. Han, T. Li, B. Gao, L. Gao, X. Tian, Q. Zhang, Y. Wang, Synergistic effects of zinc oxide in montmorillonite flame-retardant polystyrene nanocomposites, J. Appl. Polym. Sci. 133 (2016) 43047.
[25] Leyu Wang, Y. Li, Na(Y1.5Na0.5)F6 single-crystal nanorods as multicolor luminescent materials, Nano Lett. 6 (2006) 1645.
[26] Y.J. Wan, L.C. Tang, L.X. Gong, D. Yan, Y.B. Li, L.B. Wu, J.X. Jiang, G.Q. Lai, Grafting of epoxy chains onto graphene oxide for epoxy composites with improved mechanical and thermal properties, Carbon 69 (2014) 467–480.
[27] M. Abdalla, D. Dean, P. Robinson, E. Nyairo, Cure behavior of epoxy/MWCNT nanocomposites: the effect of nanotube surface modification, Polymer 49 (2008) 3310–3317.
[28] B. Kaffashi, A. Kaveh, O.M. Jazani, M.R. Saeb, Improving rheological properties of covalently MWCNT/epoxy nanocomposites via surface re-modification, Polym. Bull. 68 (2012) 2187–2197.
[29] V. Eskizeybek, A. Avci, A. Gülce, The Mode I interlaminar fracture toughness of chemically carbon nanotube grafted glass fabric/epoxy multi-scale composite structures, Compos. Appl. Sci. Manuf. 63 (2014) 94–102.
[30] J. Liu, J. Tang, X. Wang, D. Wu, Synthesis, characterization and curing properties of a novel cyclolinear phosphazene-based epoxy resin for halogen-free flame retardancy and high performance, RSC Adv. 2 (2012) 5789–5799.